Development, Characterization, and Preclinical Evaluation of Dasatinib and Hesperidin Loaded Nano formulation for Cancer

Moinuddin[1*], Neekhra Sachin[2], Pasha Saeem[3], Singh Anu T[1], Jaggi Manu[4], Mani Kamaraj[1], Swarnkar SK[5]

1. **Dabur Research Foundation, Ghaziabad, India**
2. **Department of Pharmacy, Maharishi University of Information Technology, Lucknow, India**
3. **JamiaHamdard, New Delhi, India**
4. **Althea DRF Life Sciences (ADLS), New Delhi, India**
5. **LBS College of Pharmacy, Jaipur, India**

***Corresponding Author:**
moinuddin.ansari1@gmail.com

Abstract:

In this study, we aimed to develop Dasatinib/hesperidin-loaded-SLNs for chronic myeloid leukaemia (CML).Dasatinib/ hesperidin loaded-SLNs were synthesized using a high-shear homogenizer and optimized by central composite design (CCD). The optimized SLNs had particle size, PDI, and average entrapment efficiency of 162.3 nm, 0.12, and 93% respectively. Therefore, by enhancing the total amount ofCompritolas well as sonication time the polydispersity was increased. Poloxamer 188 content had a significant influence in decreasing the polydispersity index and the entrapment efficiency (EE) of the SLN was found to be 93%. Through TEM, SEM, FTIR, DSC, and HPLC analysis, SLNs were characterized, and their anticancer efficiency was assessed in both in vitro and in vitro cell viability tests (MTT).SLNs containing dasatinib and hesperidin have a round and spherical shape with a diameter of 200 nm, which is shown in figure 2. DSC and FTIR tests showed compatibility between the drugs and excipients. The drug release from optimized SLN formulation was under observation for 48 hrs. Approximately, it was observed that 30% of the drug release was done in the first 4 h and remaining 76% of the founded to be released in the last of 48 h, performing a sustained drug release pattern of the drug. According to the IC50 values determined by an independent study, Dasatinib, Hesperidin, and SLN were 33.97 µg/ml, 5158 µg/ml, and 4.03 µg/ml, respectively. A comparison of SLN and free drugs revealed that SLN was more effective at cytotoxicity. In this study, Dasatinib and hesperidin-loaded SLNs for chronic myeloid leukaemia (CML) against HL60 human leukemia cell lines were prepared using a novel formulation approach free of toxic excipients.

Keywords: chronic myeloid leukaemia (CML), dasatinib, Hesperidin, Oral bioavailability, SLN, HL60 human leukemia cell lines.

DOI Number: 10.48047/nq.2022.20.19.NQ99271 NeuroQuantology2022;20(19): 3113-3128

Introduction

The myeloproliferative neoplasm (MPN) referred to as chronic myeloid leukemia (CML) andfounded to have an incidence of 1-2 cases per 1,00, 000 individuals(1)(2). It is characterized by mutations to the hematopoietic system as well as lower production of healthy hematopoietic cells. These mutations cause the cells to proliferate or accumulate by preventing cell differentiation. In the United States, around 50% of CML patients are asymptomatic and

are generally detected through a routine medical evaluation or medical tests(3). Three phases of CML can be distinguished: the accelerated phase (AP), the chronic phase (CP), and the blast phase (BP). Most patients (90–95%) manifest with chronic myeloid leukemia chronic phase (CML-CP)(4). Advances in targeted therapies via using selective protein kinase inhibitors have shown a significant impact on the treatment of various human malignancies, in which these agents prompt major clinical responses with significantly fewer adverse effects in comparison to conventional cytotoxic chemotherapy(5)(6). As a result, prognostic stratification and treatment options have been improved. Thus, novel targeted therapies for chronic myeloid leukemia (CML) have received major attention in recent years(7)(8)(9).

Dasatinib is a second-generation Tyrosine Kinase inhibitor (TKI) that is taken orally and has antiproliferative activity against chronic myeloid leukemia (CML)(10). In the case of resistance to imatinib, it can also be used as an alternative to imatinib therapy. The action of dasatinib is 325 times more efficient than that of imatinib against unmutated BCR-ABL, and it has antagonistic effects against most imatinib-resistant mutants of BCR-ABL, and survival of cancer cells and reducing vascular permeability(11)(12)(13).On other hand, drawbacks ofdasatinib are reportedsuch as pH-dependent solubility (205 g/mL at pH 4.27 and < 1 g/mL at pH 6.98), poor absorption, and significant first-pass effect, which result inoral bioavailability of only 14–34%(14)(15). Furthermore, particular individuals may be at risk of experiencing therapeutically relevant toxicity due to the increased of dasatinib dose(13). Hence, new nanoformulations of dasatinib are required for improved oral bioavailability.

Studies have shown that consuming flavonoid-rich diets prevent several chronic diseases and cancer too, resulting in consuming flavonoid-rich supplements as food to treat cancer(16). There is an urgent need for novel effective therapeutics and treatment strategies due to the continuously increasing global prevalence of malignancies(17). A safe natural compound such as Hesperidin, which shows strong anticancer properties, may open up new possibilities in cancer treatment. In multiple preclinical studies, it has been demonstrated that it protects against malignant transformation and progression(18)(19). Hesperidin can alter tumor cell survival, division, and death mechanisms. Nevertheless, hesperidin does not have wide clinical use due to its decreased solubility in water(20). As a result, researchers are focusing on overcoming this problem by developing appropriate delivery systems for hesperidin.

Solid lipid nanoparticles (SLNs) are composed of essential solid lipid core holding a monolayer surfactant shell. In comparison, SLNs were founded to be a safer option in contrast with othernanosystems(21). They tend to overcome some major pitfalls such as poor stability &lower loadingcapacity generally encountered with liposomes, &very possible biotoxicity as well as residualorganic solvent accompanying with polymeric nanoparticle (22). Because of its lipidic components, SLNfound to solubilize highly-lipophilic drugs, and have the benefit to hold them in a much better stable suspension, evadingusage of large quantity of surfactants and helps in enhancing biopharmaceuticalperformance after various administration routes.Moreover, SLNs allow the drugs to be targeted via lymphatic system, concluding in various aids for instance protection from hepatic first-pass metabolism, enhanced drug bioavailability and reduced hepatotoxicity(23).

In this study, we specifically aimed in developing stable dasatinib and hesperidin-loaded SLNsfor chronic myeloid leukemia (CML) using a high-shear homogenizer method. To our best knowledge, none of the previous studies have detailed the usage of coloaded nanocarriers in this way.In contrast, dasatinib and hesperidin SLNs were effectively fabricated and optimized via using central composite design (CCD) with systemic characterization for entrapment efficiency (EE%), zeta potential, particle size, FTIR, SEM, XRD, TEM, and *in vitro* drug release.

Moreover, HPLC method development and MTT assay were conducted.

Materials and Methods

Materials

The precirol ATO and Compritolwere purchased from Gattetosse(Saint-Priest, France), poloxamer188 was purchased from CDH(New Delhi, India), Hesperidin was purchased from Wuhan amino acid biochemicals (Wuhan, China), and Dasatinibwas provided by Dr. Reddy's Laboratory Ltd (Hyderabad, India). Other materials used in this study were of standard analytical quality (HPLC grade).

Preparation of SLN:

SLN was prepared using the high-shear homogenizer method. Briefly, 0.2-1.5%(w/v)Compritol-188 was melted at 50 °C (oil phase). Then, dasatinib and hesperidin were added to this oil phase and stirred on a magnetic stirrer (Remi Instruments Ltd., Mumbai, India) at 600 rotation per minute (rpm) for about 15 mins. Obtained emulsion was injected into a 100 ml aqueous solution containing 5 % (w/w) poloxamer 188 while being homogenized (IKA T 25D, Germany) at 20,000 rpm for 10 min & was sonicated using a probe sonicator to obtain the desired nanoscale(24).

Experimental Design for the optimization of SLN:

Central composite design (CCD) (Design Expert® software, version 13)was used to optimize the dasatinib/hesperidin-loaded SLN. The experimental design for formulation development is the fundamental factor for constructing the preliminary screening of the experiment. For the optimization of the process, a twenty-run, 3-factor, 3-level central composite design was utilized to reduce the number of runs with 3/4 variables. Using Design-Expert Software 13th, we were able to examine the quadratic response surface as well as constricting second-order polynomials. Using the replicated center point and a set of midpoints of the edge of a multi-dimensional cube, this well-defined region of interest. This allowed us to assess main effects & interactions of the formulation ingredients used, as well as permit us to optimize the formulation.(25) Based on the design, a linear quadratic model was produced, as shown in Table 1.

Table :1 CCD independent variables with dependent variables and their actual levels with their constrains.

FactorsCoded Levels			
Independent variable	**Low (-1)**	**Medium (0)**	**high(+1)**
X_1= Campritol (%)	0.2 0.85	1.5	
X_2= Poloxamer (%)	1	3	5
X_3=Sonication time (min)	1	5.5	10
Dependent variables		**Constraints**	
Y_1= Particle Size (nm)		(100-200)	
Y_2= Polydispersity Index (PDI)		Minimum	
Y_3= Average Entrapment Efficiency(%)		Maximum	

Analysis of experimental data using Design Expert

Analysis of experiment results was carried out using DesignExpert software (13^{th}), providing valuable information, and reinforcing statistical design's utility. In Table 2, we looked at the effects of Compritol, Poloxamer 188, & sonication time on the entrapment efficiency, particle size and polydispersity index (PDI)(26).

On the basis of estimated statistical parameters like adjusted multiple coefficient,

predicted residual sum of squares andmultiple correlation coefficient were generated by Design-Expert Software, polynomial equations were generated that involveskey effect & interaction factors. Using, ANOVA provision in the software, we validated polynomial equation statistically.

Physical Characterization of SLN

Particle size, Polydispersity Index, and Zeta potential

Suitable dilutions of nanodispersion were performed with water for zeta potential, size determination, as well as PDI measurement at 25±1°C by using Nano ZS (Malvern Instruments Ltd., Worcestershire, UK)(27).

Morphology studies

Transmission Electron Microscopy (TEM)

The optimized SLN was diluted 10 times with Milli Q water before placing a drop of the sample solution onto the cu-grid and allowing it to dry at room temperature. The prepared sample was stained with 1% phosphotungstic acid for better visibility, and the TEM photomicrographs were taken with the ((TEM) (Tecnai G2 S-twin, FEI, Netherland) instrument(28).

Scanning Electron Microscopy (SEM)

Took an appropriate amount of optimized sample solution and placed a drop on a carbon-coated Cu-grid using a gold sputter module in a high vacuum evaporator. SEM photomicrographs were taken at an exciting voltage of 10Kv using the (SEM) (EVO LS 10 Zeiss, Carl Zeiss INC., Germany)(29).

Physiochemical characterization

Fourier Transform Infrared Spectrophotometric (FTIR) analysis

To investigate the drug-polymer interactions, an appropriate number of samples were analyzed, and the %transmittance was recorded using the FTIR (FTIR, Nicolet iS5) instrument in a scanned range of 400-4000 cm^{-1}(30).

Differential scanning calorimetry (DSC) analysis

Five milligrams(5mg) of drug sample were accurately weighed &put in the hermetically sealed aluminum (Al) DSC pan. Further, the pan was sealed using hydraulic press. The sample was scanned within the temp. range of 40-400°C with given (10°C/min) heating rate. This study was executed using the Differential scanning calorimeter (DSC), model DSC6 instrument.

HPLC analysis

The RP-HPLC was used for the quantification of hesperidin and dasatinib by using the zorbax eclipse xdb c-8 (250 x 4. 6 mm, 5µm particle size) or equivalent with given (1.0 ml/min) flow rate with a column oven temperature of 30 °C. The mobile phase was a mixture of methanol and phosphate buffer (2.75 g potassium dihydrogen phosphate KH_2PO_4 in 1000 ml milli-Q water) (48:52) & the pH was adjusted to 4.5. After 15 minutes, the 10µl samplewas injected and scanned at 280 nm and 323 nm(31).

Preparation of standard: 1000 ppm was achieved by taking the 10mg in a 10 mL standard flask, with the remaining volume being made up with DMSO. For further dilution use methanol. Vortex the sample for 10 mins and then sonicate for 10 mins. Filter and inject the samples onto HPLC

Preparation of sample: Added 1 mL of DMSO to 500 mg of sample in a 2 mL Eppendorf tube. Vortex, sonicate, and centrifuge for 10 minutes at 14000 rpm as previously mentioned. Next, add another 1 mL of DMSO to 1 mL of the supernatant layer. The same procedures were used for centrifuging, sonicating, and vortexing. injected the filtered upper layer into the HPLC after taking it.

Encapsulation Efficiency

1 mL of DMSO was added to 500 mg of the sample in a 2 mL Eppendorf tube. Centrifuge the sample solution for 10 minutes followed by a vortex and sonication. Then took the supernatant layer of about 1 mL and further added 1 mL of H2O. Followed the same for vortexing, sonication, and centrifuging. Took the upper layer, filter it, and inject it onto HPLC for analysis.

***Invitro* Drug release**

Invitro drug release of the optimized formulation was evaluated for 24 h of preparation under the sink conditions. Briefly, add the optimized SLN dispersion to the dialysis bag and sealed both ends, placed the bag in the beaker containing the Phosphate buffer (pH 6.8) on the magnetic stirrer at a controlled temperature of 37 ± 0.5°C with 100

rpm of speed. After the different time intervals, 0, 0.25, 0.5, 1, 2, 4, 6, 8, 12, 24hrs, samples were withdrawn and analyzed by HPLC(32).

***In vitro* cell viability assay (MTT assay)**

Cell viability testing was done using MTT on the HL60 Human leukemia cell line to observe the cytotoxic potential of dasatinib and hesperidin-loaded solid lipid nanoparticles. Briefly, cells were seeded in a 96-well flat-bottom microtiter plate at a density (ρ) of 1104 cells/well & incubated for 36 h to grow & attach(33). Afterward, dasatinib and hesperidin-loaded solid lipid nanoparticles were added at different concentrations (50 µg to 0.1 µg/ml) and incubated for 36 h. After 36 h, medium was superseded with fresh medium &furthermore, the cells were incubated with 20 µl of MTT (5 mg/ml in PBS) for 4 h at 37°C. Moreover, Formazan crystals were dissolved in Dimethyl sulfoxide (DMSO), which was further produced via mitochondrial reduction of MTT (150 L/well) & was computed by reading the absorbance at 540 nm on the Mark microplate reader (Bio-Rad) below equation was used for the calculation(34)

$$\%\text{Viable cells} = (Abs_{sample} - Abs_{blank})/(Abs_{control} - Abs_{blank}) * 100\%$$

Result & Discussion

Preparation of SLN by CCD approach

20 experimental runs, 3 levels of central composite design were employed to buildthe polynomial models for optimization of formulation as mentioned in Table 2.(35)

Table: 2 Composition of 3 factors, 3 levels CCD for the formulation development

Run	A: Solid Lipid %(w/w)	B: Surfactant %(w/w)	C: Sonication Time(min)	Response 1 Particle Size	Response 2 PDI	Response 3 %EE
1	0.85	3	5.5	162.3	0.125	93
2	0.85	3	5.5	162.3	0.125	93
3	1.5	3	5.5	233	0.631	71
4	0.85	5	5.5	162.3	0.125	93
5	0.2	3	5.5	198	0.345	85
6	0.85	3	1	145	0.456	91
7	0.85	1	5.5	152	0.378	92
8	0.85	3	5.5	162.3	0.125	93
9	1.5	5	1	264	0.561	72
10	0.85	3	10	179	0.621	79
11	0.2	1	1	153	0.561	87
12	0.2	5	1	189	0.521	83
13	0.2	5	10	167	0.815	58
14	1.5	1	10	189	0.767	76
15	1.5	1	1	167	0.614	67

16	0.85	3	5.5	189	0.125	93
17	0.2	1	10	156	0.843	88
18	0.85	3	5.5	162.3	0.125	93
19	0.85	3	5.5	162.3	0.125	93
20	1.5	5	10	265	0.934	68

Physical Characterization of SLN

Effect of the variable on particle size (Y_1)

As per the obtained result of the experiments, particle size ranged from 145 to 265 as shown in Table 2. The amount of Compritol had an effect on the size. Following mentioned equation can elaborate effect of factor levels on particle size:

Particle Size (Y1) +179.74.60= 19.11A+5.75B-1.47C+22.68AB+3.00AC+0.377BC-8.21A^2 - 7.41B^2 -14.84C^2

The main effect of Y_1, Y_2, and Y_3 represents average result of altering 1 variable at a time from its lower level to its higher level. The positive coefficients show us a favorable effect on size. Whereas, negative coefficients before independent variables are indicating an unfavorable effect on the size. Investigating these mentioned coefficients in the above 2ndorder polynomial mode is shown in Figure 1(i) graph.

Moreover, modelF-value for full quadratic particle size of nanoparticles was 20.69, indicating the linear response surface and quadratic model was significant as mentioned in Table 3. By analyzing responses surfaces predicted particle size as shown in Figure-1 (a) that an increase in Poloxamer 188 leads to a decrease in particle size(36).

Effect of the variable on Poly Dispersity Index (Y_2)

As per the obtained results from the experiments, the particle size value varies from Poly Dispersity Index **(**PDI) 0.125 to 0.934 as mentioned in Table 2. The small value of PDI was highly desirable to have even size distribution in the dispersion media. PDI was influenced by the amount of Compritol& Sonication time. Below mentioned equation shows the relationship between the above mention factors & PDI.

Poly Dispersity Index (Y2) +0.3575= -0.0822A-0.1693B-0.0040C+0.1524AB+0.0894AC+0.0004BC-0.0581A^2 +0.3830B^2 -0.1594C^2

The "Model F-value" of 14.00 implies the model is significant as mentioned in Table 3. There was only a 0.05% chance that a "Model F-value" this larger could occur due to noise. Figure 1 (ii) showed the influence of different variables on PDI. On increasing the amount of Compritol and sonication time the polydispersity was increased. Poloxamer 188 content had a significant influence in decreasing the polydispersity index.

The Effect on Encapsulation Efficiency (Y_3)

Encapsulation Efficiency willdemonstrate the preparative efficiency of Compritol formulation. For EE, p-values of X_1 (Compritol), X_2 (Poloxamer 188), and X_3 (Sonication time) were all < 0.0001, signifying that these variables hadnoteworthy differences in the EE response as mentioned in Table 3. Encapsulation efficiency might get reduced with higher Compritol concentration & lesser quantity of Cholesterol +Stearic acid. Following equation showedthat the relationship between above mention factors & Encapsulation Efficiency(35).

Encapsulation Efficiency (Y3) +88.2= 3.18A-3.60B+5.61C-5.25AB-7.00AC+1.25BC-3.80A^2 - 10.57B^2 -5.49C^2

The "Model F-value" of 8.53 infers the model wasvital. There was only 0.15% chance that a "Model F-value" could be this large due to noise. Figure 1 (iii) showed the influence of different variables on entrapment efficiency. On enhancing the quantity of Compritol& sonication time the entrapment efficiency was decreased. Surfactant contents did not have a significant influence in increasing the entrapment efficiency.

Table 3: ANOVA results for Quadratic model

Response	F-value	P-value	Mean square	AdjustedR^2	PredictedR^2	Remarks
Particle size (Y1)	20.69	<0.0001	2455.77	0.9032	0.6102	Significant
Poly Dispersity Index (Y2)	14.00	<0.0001	0.1540	0.8603	0.4838	Significant
Encapsulation Efficiency (Y3)	22.35	<0.0001	245.87	0.9100	0.5098	Significant

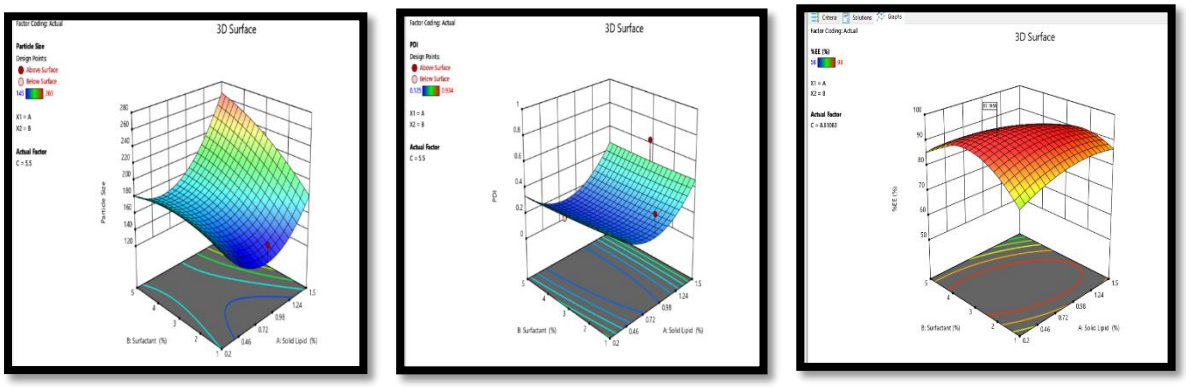

Figure:1 Response surface plots of (i) particle size, (ii) Poly Dispersity Index, and (iii) Encapsulation Efficiency

Particle size and Polydispersity Index.

As shown in Table 2, all formulations ranged in particle size from 145 to 265 nm and PDI from 0.125 to 0.934. This optimized formulation showed particle size in a range of 162.3 nm with PDI of 0.12, as shown in figure 1.

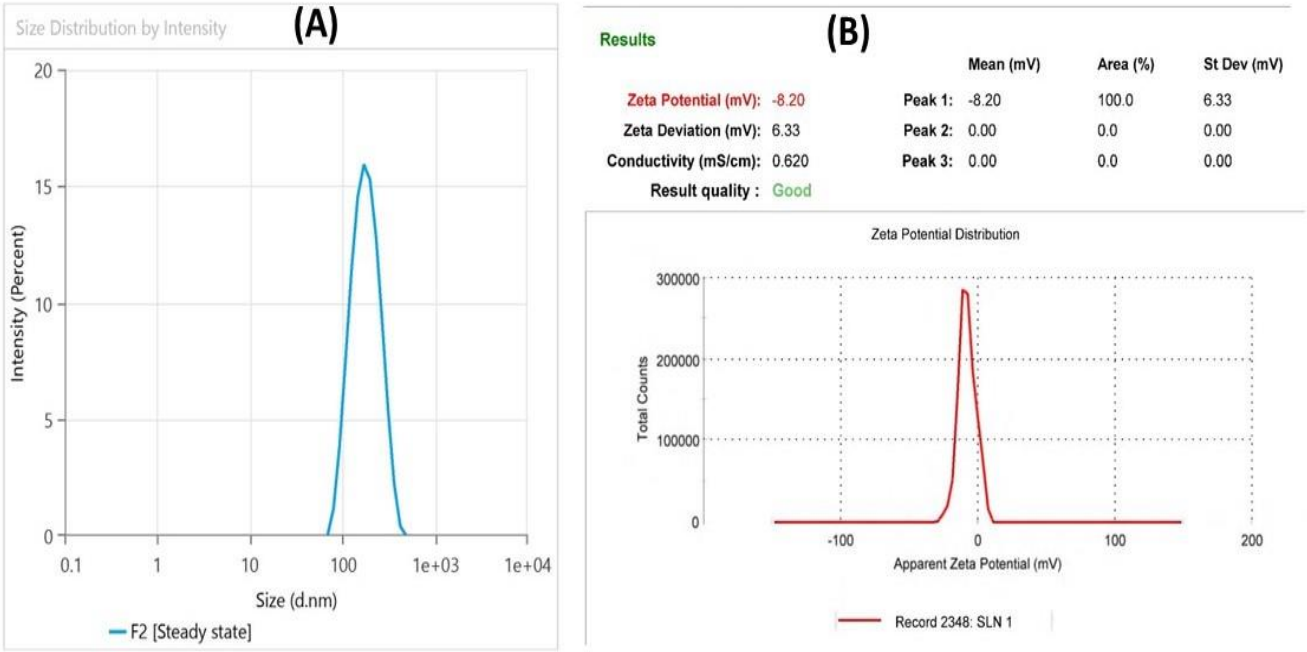

Figure 2: (A) Particle size and (B) zeta potential of the optimized dasatinib-hesperidin SLN.

Morphology studies

Scanning Electron Microscopy (SEM) & Transmission Electron Microscopy (TEM) were

utilized for studying morphology of dasatinib and hesperidin-loaded SLN, showed a round and spherical shape with 200 nm in diameter as mentioned in figure 2.

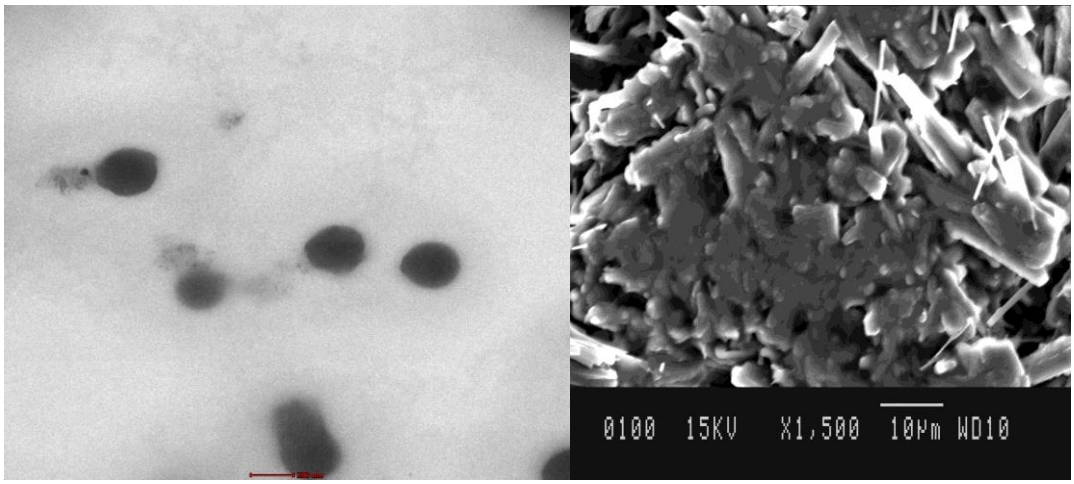

Figure 3: SEM and TEM analysis

Physiochemical characterization

Fourier Transform Infrared Spectrophotometric (FTIR) analysis

FTIR spectra of Drugs (dasatinib&hesperidin), and a mixture of drugs are mentioned in Figure 3, other IR spectra of dasatinib-excipients mixtures are mentioned in figure 4 and IR spectra of hesperidin-excipients mixtures are mention in Figure 5 and the final spectra of SLN formulation is mention in Figure 6.

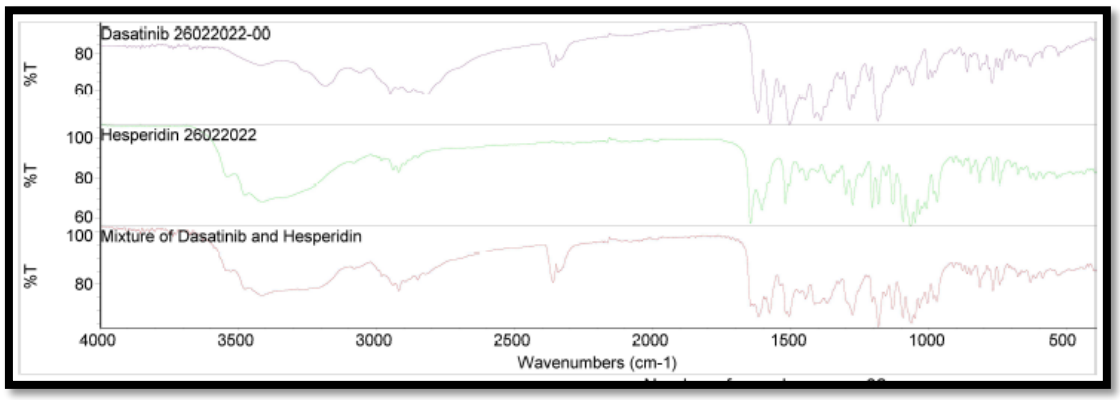

Figure 4: FTIR Spectrum of Dasatinib, Hesperidin, and mixtures

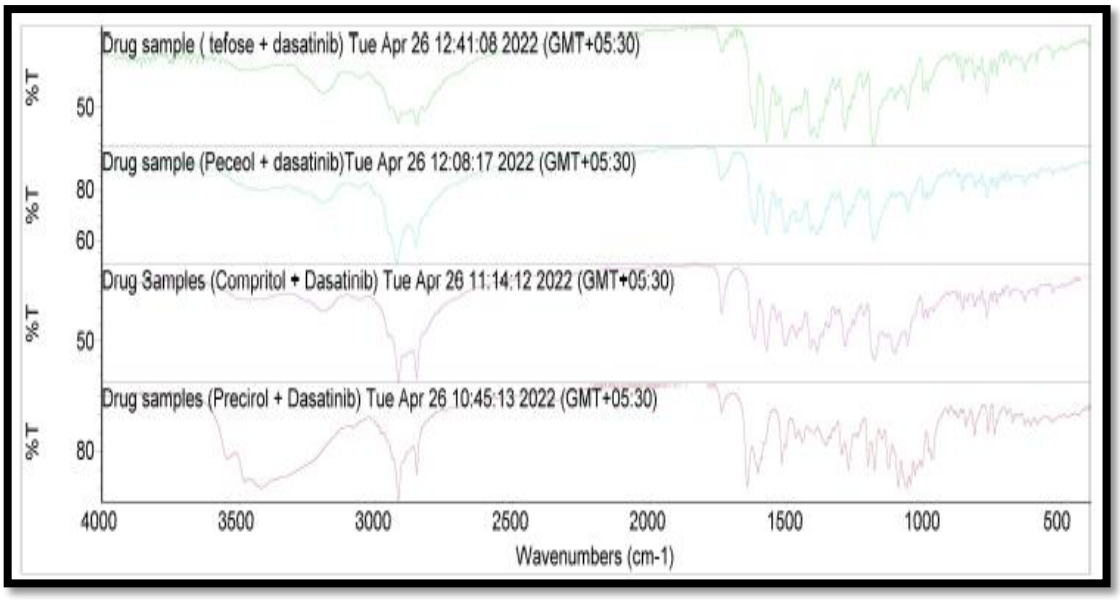

Figure 5: FTIR Spectrum of Dsatinib and Excipients

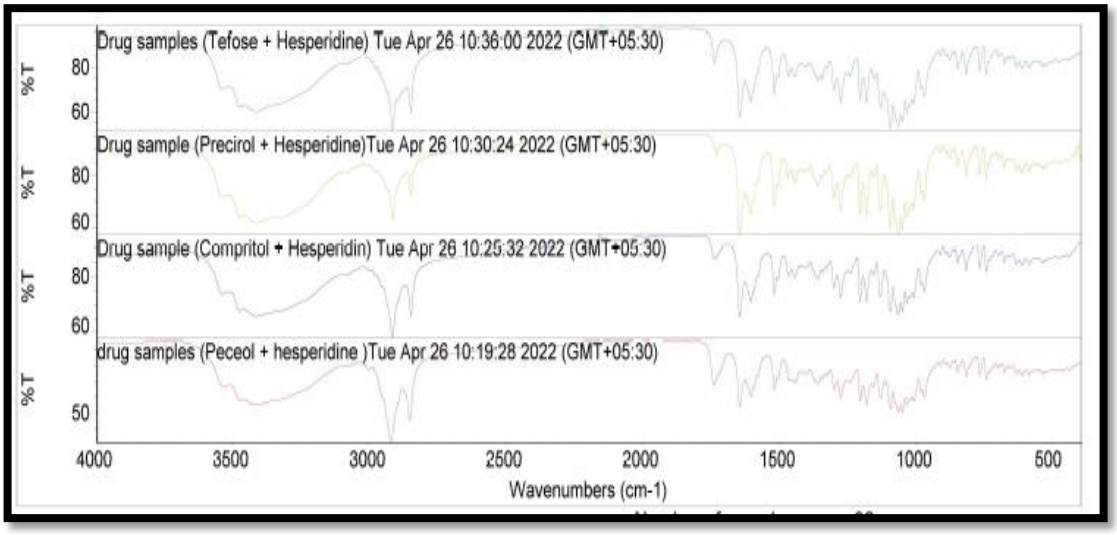

Figure 6: FTIR Spectrum of Hesperidin and Excipients

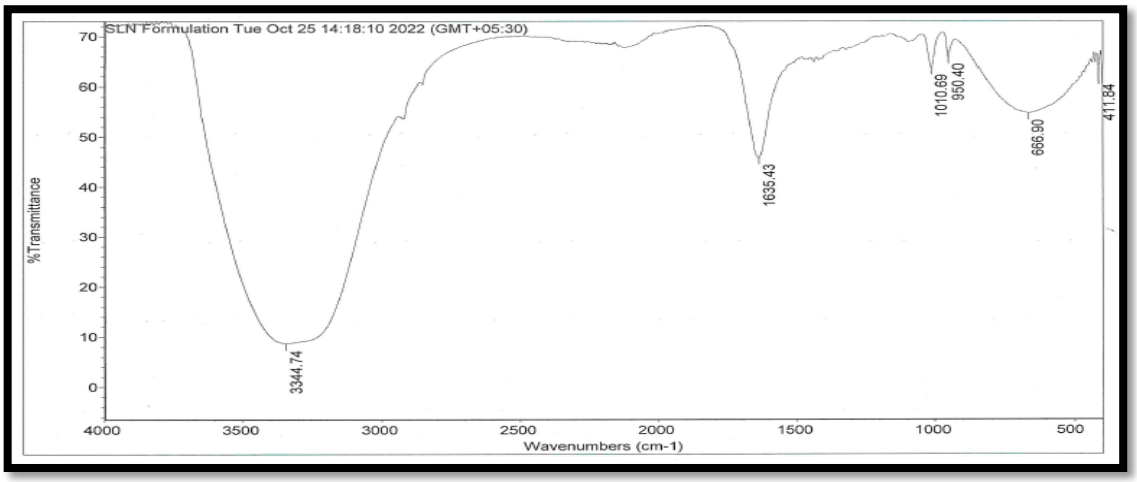

Figure 7: FTIR Spectrum of SLN

Differential scanning calorimetry (DSC) analysis

The endotherm of Dasatinib, Hesperidin, and optimized SLN and their typical curve is shown

in figure 7. The absence of Dasatinib& Hesperidin peaks in optimized SLN formulation indicates that the drug was successfully loaded in the lipid core.

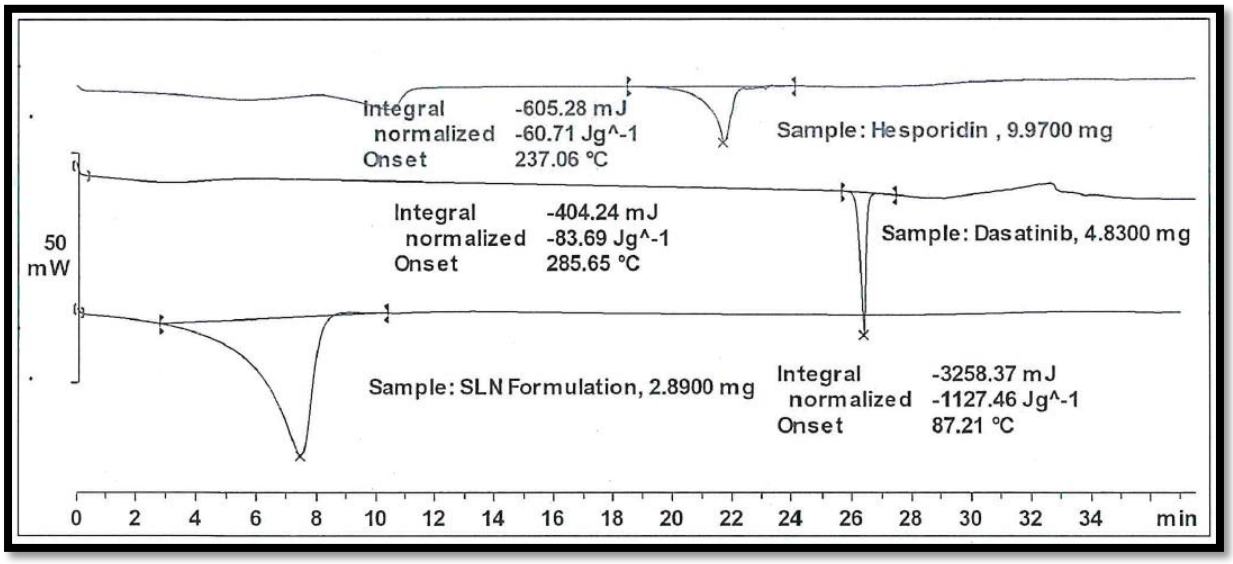

Figure 8: DSC Analysis

HPLC analysis

The calibration curve for Dasatinib& Hesperidin was constructed by plotting the concentration versus peak area (Fig 8 (a & b)). The response was a linear function of Dasatinib concentration (R>) in the range of 25-300 (µg/ml) (Fig 8(a)). The regression equation for the calibration plot was y= 0.7457x+0.3610, detected at 323 nm (Table 4 (a)). The representative linear regression equation for Hesperidin was y= 0.22x+0.04 (Table 5 (b)) in the range of 25-300 (µg/ml) (Fig 8). There was no major difference was observed between the slopes of calibration plots as mentioned in the integrated results in Figure 9(37).

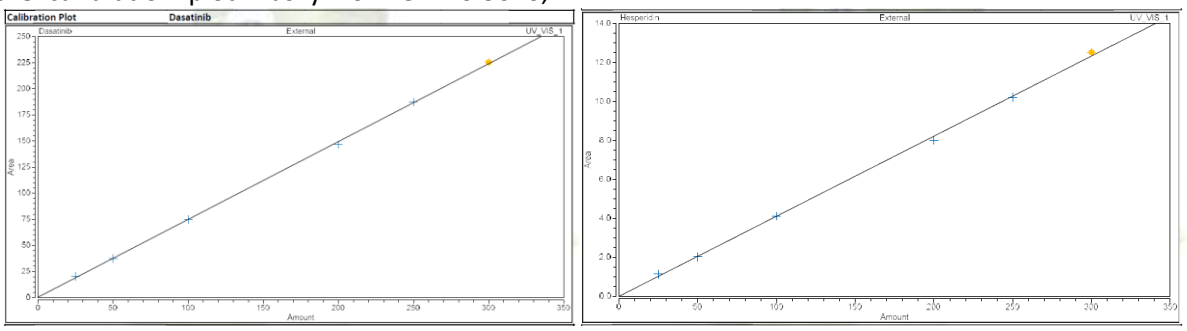

Figure 9: Typical HPLC chromatogram of Dasatinib using a UV-visible detector at 323 nm

Table 4: Linear regression data for (a) Dasatinib& (b) Hesperidin calibration curves

Concentration (mg/L) Dasatinib	**Peak Area (Y)**
24.95	20.294
49.90	37.408
99.80	74.752
199.60	146.665
249.50	187.316
299.40	225.537
Intercept (a)	0.36
Slope (b)	0.75

R	0.99983

Concentration (mg/L) Hesperidin	**Peak Area (Y)**
25.00	5.967
50.00	10.689
100.00	21.723
200.00	42.120
250.00	53.732
300.00	65.778
Intercept (a)	**0.04**
Slope (b)	**0.22**
R	**0.99957**

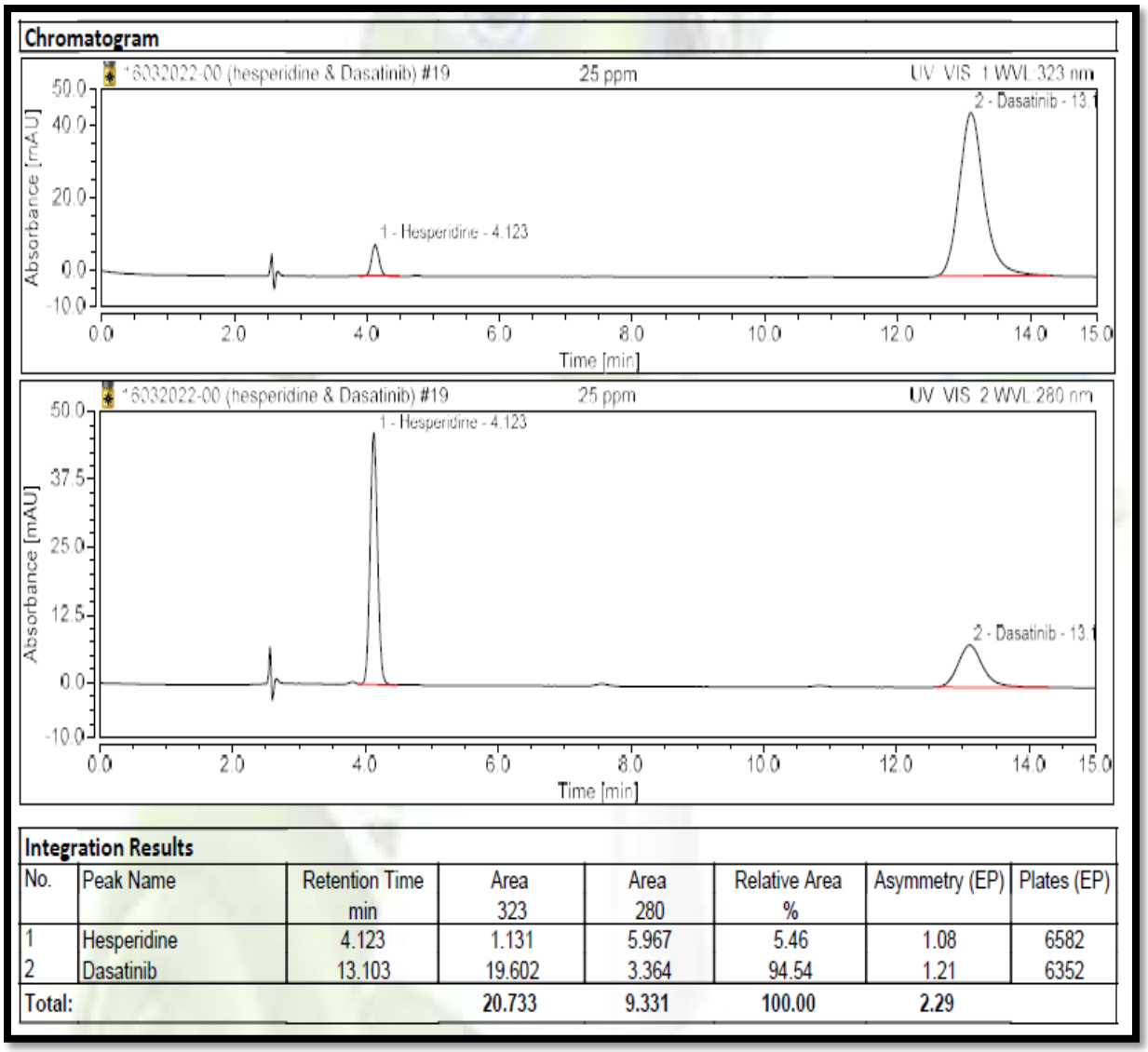

Integration Results

No.	Peak Name	Retention Time min	Area 323	Area 280	Relative Area %	Asymmetry (EP)	Plates (EP)
1	Hesperidine	4.123	1.131	5.967	5.46	1.08	6582
2	Dasatinib	13.103	19.602	3.364	94.54	1.21	6352
Total:			20.733	9.331	100.00	2.29	

Figure 10: Integrated Results

***Invitro* Drug release**

Releasing pattern of the optimized SLN formulation and suspension is shown in Figure 9. The results showed that for dasatinib and hesperidin, 45.5 percent and 31.4 percent of the drugs were released from the SLN in the first 4 hours, respectively, while 66.5 percent and 51.8 percent of the drugs were released in the concluding 24 hours. Representing burst release of drugs adsorbed on the surface of SLNs, followed by sustained drug release, confirming that the drugs were encapsulated in the lipid core. *In vitro* drug release profile data was fitted to Higuchi square root (R^2 0.6624), Hixon–Crowell cube root (R^2 0.7642), Korsmeyer–Peppas (R^2 0.9909) zero-order (R^2 0.6624) and first-order (R^2 0.6624) kinetic models. Kinetic modelingof drug release of the optimized SLN formulation was explained thoroughly by the Korsmeyer–Peppas model (highest R^2)(38).

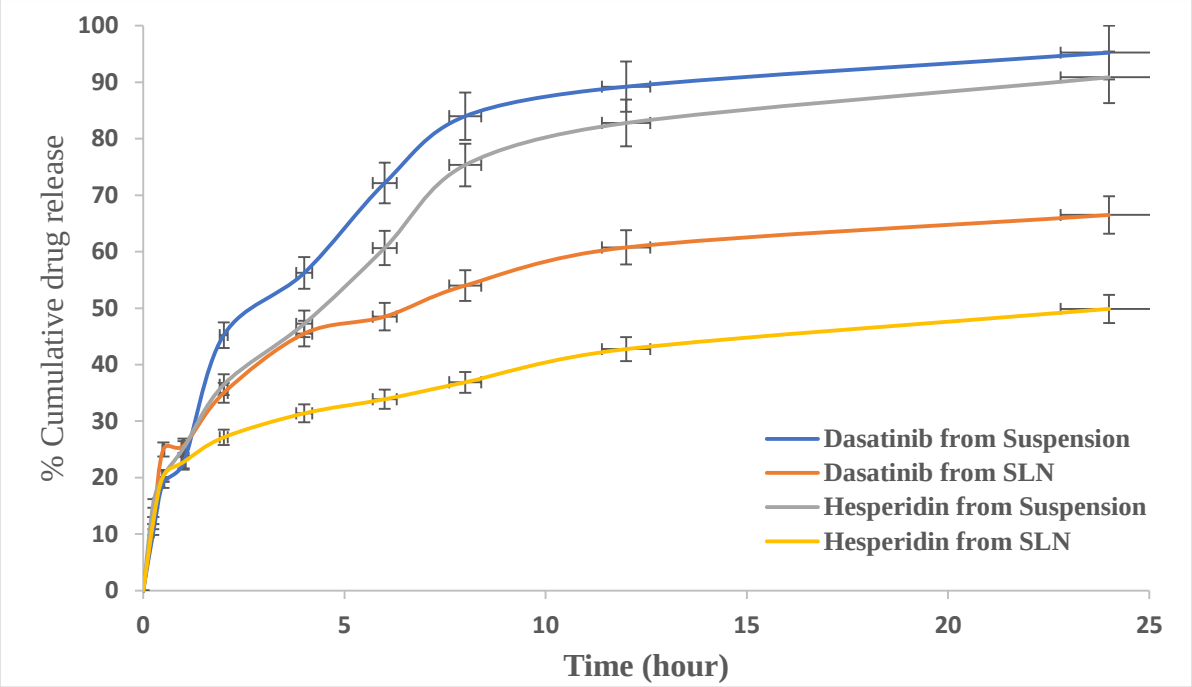

Fig. 11. In vitro drug release profiles of dasatinib and hesperidin from suspension and SLNformulations.

***In vitro* cell viability assay (MTT assay)**

As shown in figure 10, free Dasatinib& Hesperidin and optimized SLN formulation showed comparable cytotoxicity outcomes against HL60 Human leukemia cell lines. According to the IC50 values determined by an independent study, Dasatinib, Hesperidin, and SLN were 33.97 µg/ml, 5158 µg/ml, and 4.03 µg/ml, respectively. A comparison of SLN and free drugs revealed that SLN was more effective at cytotoxicity.

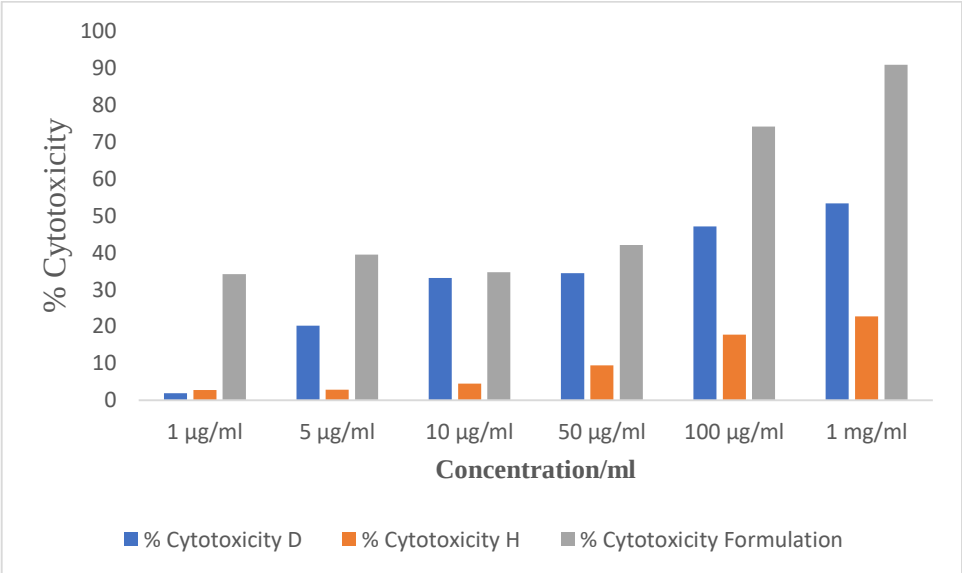

Figure 12: In vitro cytotoxicity of Dasatinib& Hesperidin and optimized SLN formulation

Conclusion

In this study, we demonstrate that high-shear homogenizers are effective for preparing SLNs containing Dasatinib& hesperidin for chronic myeloid leukemia (CML), which enhanced the cytotoxicity and stability of Dasatinib and hesperidin while reducing the associated toxic effects. Based on the 20 run experiments, the optimized formulation demonstrated particle size in a range of 162.3 nm, with a PDI of 0.12, with a narrow size distribution. In addition, they were able to release both Dasatinib and

Hesperidin in a sustained manner, demonstrating the fact that the drugs were encapsulated in the lipid core. There was a 93% entrapment efficiency (EE) for the SLN. Each of the 3 variables X_1 (Compritol), X_2 (Poloxamer 188), and X3 (Sonication time) had a p-value equivalent to less than 0.0001, suggesting significant differences in particle size, PDI, and EE%. TEM and SEM analysis of dasatinib- and hesperidin-loaded SLN revealed a round and spherical shape with a diameter of 200 nm and physical compatibility. HL60 cells showed comparable cytotoxicity againstdasatinib and hesperidin when combined with the optimized SLN formulation. A study conducted independently determined the IC50 values for Dasatinib, Hesperidin, and SLN as 33.97 g/ml, 5158 g/ml, and 4.03 g/ml, respectively. A comparison of SLN and free drugs revealed that SLN was more effective at cytotoxicity. Therefore, the developed dual-targeted Dasatinib&Hesperidin demonstrated higher sensitivity of cells to the drug entrapped in SLN than the drug solution. This novel approach may result in improved prognosis with an improvement in the life quality of patients as a result of the development of sustained release formulations of anticancer drugs.

Disclosure statement

The authors declare no conflict of interest.

Acknowledgment

References

1. Htun HL, Lian W, Wong J, Tan EJ, Foo LL, Ong KH, et al. Classic myeloproliferative neoplasms in Singapore: A population-based study on incidence, trends, and survival from 1968 to 2017. Cancer Epidemiol. 2022 Aug 1;79:102175.
2. Katogiannis K, Ikonomidis I, Panou F, Katsimardos A, Divane A, Tsantes A, et al. Leukostasis-Related Fatal Cardiopulmonary Arrest as Initial Chronic Myeloid Leukemia Presentation. J Med Cases. 2018;9(3):77–82.
3. Jabbour E, Kantarjian H. Chronic myeloid leukemia: 2018 update on diagnosis, therapy and monitoring. Am J Hematol. 2018;93(3):442–59.
4. Jabbour E, Kantarjian H. Chronic myeloid leukemia: 2020 update on diagnosis, therapy and monitoring. Am J Hematol. 2020;95(6):691–709.
5. Vanneman M, Dranoff G. Combining immunotherapy and targeted therapies in cancer treatment. Nat Rev Cancer. 2012;12(4):237–51.
6. Smyth LA, Collins I. Measuring and interpreting the selectivity of protein kinase inhibitors. J Chem Biol. 2009;2(3):131–51.
7. Hu J, Xing K, Zhang Y, Liu M, Wang Z. Global Research Trends in Tyrosine Kinase Inhibitors: Coword and Visualization Study. JMIR Med Inform. 2022;10(4):1–18.
8. Lopina N, Dmytrenko I, Hamov D, Lopin D, Dyagil I. A New Paradigm of Cardio-Hematological Monitoring in Chronic Myeloid Leukemia Patients Treated With Tyrosine Kinase Inhibitors. Cureus. 2022;14(6):5–14.
9. Jim HSL, Hyland KA, Nelson AM, Pinilla-Ibarz J, Sweet K, Gielissen M, et al. Internet-assisted cognitive behavioral intervention for targeted therapy–related fatigue in chronic myeloid leukemia: Results from a pilot randomized trial. Cancer. 2020;126(1):174–80.
10. Bahman F, Pittalà V, Haider M, Greish K. Enhanced anticancer activity of nanoformulation of dasatinib against triple-negative breast cancer. J Pers Med. 2021;11(6).
11. Yang, S.X., & Dancey JE. Handbook of Therapeutic Biomarkers in Cancer. 2nd Editio. New York: Jenny Stanford Publishing; 2021.
12. Wolfe, H.R., Rein LAM. The Evolving Landscape of Frontline Therapy in Chronic Phase Chronic Myeloid Leukemia (CML). Curr Hematol Malig Rep. 2021;16:448–54.
13. He S, Bian J, Shao Q, Zhang Y, Hao X, Luo X, et al. Therapeutic Drug Monitoring and Individualized Medicine of Dasatinib: Focus on Clinical Pharmacokinetics and Pharmacodynamics. Front Pharmacol. 2021;12(December):1–11.

14. Arafath, A. A. M. Y. ., & Jaykar B. Determining the Enhancement of Oral Bioavailability VIA Solid Lipid Nanoparticles of Anticancer Drug Dasatinib - An In-vitro Cytotoxicity and Pharmacokinetic Study. Curr Asp Pharm Res Dev. 2021;2:161–8.
15. Dharani S, Mohamed EM, Khuroo T, Rahman Z, Khan MA. Formulation Characterization and Pharmacokinetic Evaluation of Amorphous Solid Dispersions of Dasatinib. Pharmaceutics. 2022 Nov 13;14(11):2450.
16. Janabi AHW, Kamboh AA, Saeed M, Xiaoyu L, BiBi J, Majeed F, et al. Flavonoid-rich foods (FRF): A promising nutraceutical approach against lifespan-shortening diseases. Iran J Basic Med Sci. 2020;23(2):140–53.
17. Alhalmi A, Amin S, Beg S, Al-Salahi R, Mir SR, Kohli K. Formulation and optimization of naringin loaded nanostructured lipid carriers using Box-Behnken based design: In vitro and ex vivo evaluation. J Drug Deliv Sci Technol. 2022;74(June):103590.
18. Aggarwal V, Tuli HS, Thakral F, Singhal P, Aggarwal D, Srivastava S, et al. Molecular mechanisms of action of hesperidin in cancer: Recent trends and advancements. Exp Biol Med. 2020;245(5):486–97.
19. Saleh N, Allam T, Korany RMS, Abdelfattah AM, Omran AM, Abd Eldaim MA, et al. Protective and Therapeutic Efficacy of Hesperidin versus Cisplatin against Ehrlich Ascites Carcinoma-Induced Renal Damage in Mice. Pharmaceuticals. 2022 Feb 28;15(3):294.
20. Sulaiman GM, Waheeb HM, Jabir MS, Khazaal SH, Dewir YH, Naidoo Y. Hesperidin Loaded on Gold Nanoparticles as a Drug Delivery System for a Successful Biocompatible, Anti-Cancer, Anti-Inflammatory and Phagocytosis Inducer Model. Sci Rep. 2020;10(1):1–16.
21. Martins S, Sarmento B, Ferreira DC, Souto EB. Lipid-based colloidal carriers for peptide and protein delivery - Liposomes versus lipid nanoparticles. Int J Nanomedicine. 2007;2(4):595–607.
22. Russo E, Spallarossa A, Tasso B, Villa C, Brullo C. Nanotechnology of tyrosine kinase inhibitors in cancer therapy: A perspective. Int J Mol Sci. 2021;22(12).
23. Emad NA, Ahmed B, Alhalmi A, Alzobaidi N, Al-Kubati SS. Recent progress in nanocarriers for direct nose to brain drug delivery. J Drug Deliv Sci Technol. 2021;64:102642.
24. Vandghanooni S, Rasoulian F, Eskandani M, Akbari Nakhjavani S, Eskandani M. Acriflavine-loaded solid lipid nanoparticles: preparation, physicochemical characterization, and anti-proliferative properties. Pharm Dev Technol. 2021;26(9):934–42.
25. Jain S, Jain S, Khare P, Gulbake A, Bansal D, Jain SK. Design and development of solid lipid nanoparticles for topical delivery of an anti-fungal agent. Drug Deliv. 2010 Aug;17(6):443–51.
26. Vaghasiya H, Kumar A, Sawant K. Development of solid lipid nanoparticles based controlled release system for topical delivery of terbinafine hydrochloride. Eur J Pharm Sci. 2013 May;49(2):311–22.
27. Sipos E, Szabó ZI, Rédai E, Szabó P, Sebe I, Zelkó R. Preparation and characterization of nanofibrous sheets for enhanced oral dissolution of nebivolol hydrochloride. J Pharm Biomed Anal. 2016 Sep;129:224–8.
28. Szabó P, Daróczi TB, Tóth G, Zelkó R. In vitro and in silico investigation of electrospun terbinafine hydrochloride-loaded buccal nanofibrous sheets. J Pharm Biomed Anal. 2016 Nov;131:156–9.
29. Wong CY, Al-Salami H, Dass CR. The role of chitosan on oral delivery of peptide-loaded nanoparticle formulation. J Drug Target. 2018 Aug 9;26(7):551–62.
30. Younes NF, Abdel-Halim SA, Elassasy AI. Corneal targeted Sertaconazole nitrate loaded cubosomes: Preparation, statistical optimization, in vitro characterization, ex vivo permeation and in vivo studies. Int J Pharm. 2018 Dec;553(1–2):386–97.
31. Yang S, Zhang X, Wang Y, Wen C, Wang C, Zhou Z, et al. Development of UPLC-

MS/MS Method for Studying the Pharmacokinetic Interaction Between Dasatinib and Posaconazole in Rats. Drug Des Devel Ther. 2021 May;Volume 15:2171–8.

32. zur Mühlen A, Schwarz C, Mehnert W. Solid lipid nanoparticles (SLN) for controlled drug delivery – Drug release and release mechanism. Eur J Pharm Biopharm. 1998 Mar;45(2):149–55.
33. Ahmad S, Khan I, Pandit J, Emad NA, Bano S, Dar KI, et al. Brain targeted delivery of carmustine using chitosan coated nanoparticles via nasal route for glioblastoma treatment. Int J Biol Macromol. 2022 Nov;221:435–45.
34. Núñez-Sánchez MÁ, Martínez-Sánchez MA, Verdejo-Sánchez M, García-Ibáñez P, Oliva Bolarín A, Ramos-Molina B, et al. Anti-Leukemic Activity of Brassica-Derived Bioactive Compounds in HL-60 Myeloid Leukemia Cells. Int J Mol Sci. 2022 Nov 2;23(21):13400.
35. Varshosaz J, Ghaffari S, Khoshayand MR, Atyabi F, Azarmi S, Kobarfard F. Development and optimization of solid lipid nanoparticles of amikacin by central composite design. J Liposome Res. 2010 Jun;20(2):97–104.
36. Hassan H, Adam SK, Alias E, Meor Mohd Affandi MMR, Shamsuddin AF, Basir R. Central Composite Design for Formulation and Optimization of Solid Lipid Nanoparticles to Enhance Oral Bioavailability of Acyclovir. Molecules. 2021 Sep 7;26(18):5432.
37. Secrétan PH, Karoui M, Bernard M, Ghermani N, Safta F, Yagoubi N, et al. Photodegradation of aqueous argatroban investigated by LC/MSn : Photoproducts, transformation processes and potential implications. J Pharm Biomed Anal. 2016 Nov;131:223–32.
38. Zhao Y, Chang YX, Hu X, Liu CY, Quan LH, Liao YH. Solid lipid nanoparticles for sustained pulmonary delivery of Yuxingcao essential oil: Preparation, characterization and in vivo evaluation. Int J Pharm. 2017 Jan;516(1–2):364–71.
39. Manda H, Swarnkar SK, Swarnkar A, Rasal AS, Shanbhag R, Kutty NG. Wound Healing Potential of PYRAZOLE DERIVATIVE. Pharmacologyonline. 2009;2(1):53–60.
40. Gupta MK, Swarnkar SK. Preformulation Studies of Diltiazem Hydrochloride from Tableted Microspheres. J Drug Deliv Ther. 2018;8(1):64–9.
41. Khunteta A, Gupta MK, Swarnkar SK. Formulation of Rapid Dissolving Films Containing Granisetron Hydrochloride and Ondansetron Hydrochloride. J Drug Deliv Ther. 2019;9(4-A):516–27.
42. Dheer R, Swarnkar SK, Syeed F. Chromatographic Analysis of Barleria prionitis Linn. Res J Pharm Tech. 2019;12(8):1–8.
43. Jain P, Jain S, Swarnkar SK, Sharma S, Paliwal S. Screening of analgesic activity of Phoenix sylvestris leaves in rodents. J Ayurvedic Herb Med. 2018;4(1):22–4. Available from:
44. Swarnkar S, Jain Y, Kumawat M, Khunteta A, Paliwal S. Exploration of autonomic involvement in mechanism of antinociceptive activity of flowering top extract of Aerva javanica. Asian J Biochem Pharm Res. 2019;(SI):33–6.
45. Laxane SN, Swarnkar SK, Setty MM. Antioxidant studies on the ethanolic extract of Zornia gibbosa. Pharmacologyonline. 2008;1(1):319–30.